Available online at www.sciencedirect.com
SCIENCE DIRECT
Polymer 46 (2005) 4776–4788
polymer
www.elsevier.com/locate/polymer

Dynamic colloidal processes in waterborne two-component polyurethanes and their effects on solution and film morphology

Daniel B. Otts, Kevin J. Pereira, William L. Jarret, Marek W. Urban*

Shelby F. Thames Polymer Science Research Center, School of Polymers and High Performance Materials, The University of Southern Mississippi, 118 College Drive # 10076, Hattiesburg, MS 39406, USA

Received 12 January 2005; received in revised form 22 March 2005; accepted 1 April 2005
Available online 22 April 2005

Abstract

While waterborne two-component polyurethanes (WB 2K-PURs) offer an attractive approach toward the reduction of volatile organic compounds (VOC), a number of fundamental processes related to the colloidal stability and solution morphology of WB 2K-PUR reactive dispersions are not understood. These studies focus on mechanisms of inter-particle reactant aggregation in heterogeneous aqueous dispersions resulting from solution morphological changes of poly(ethylene glycol) modified water-dispersible polyisocyanates (WDPI) and water-reducible polyester polyol coreactants, as revealed by particle size measurements and in situ NMR T_2 studies. Based on the results of these experiments, a model of film formation is proposed which relates solution morphological features and chemical reactions. WDPI reactant droplets become hydrated over time, leading to formation of carbon dioxide, which dissolves in the aqueous continuum as carbonic acid and subsequently destabilizes anionically stabilized polyol droplets, resulting in their adsorption to WDPI droplet surfaces. The implications of polyol collapse, as they pertain to film formation, are discussed in the context of solution and film morphologies.

Keywords: Waterborne two-component polyurethanes; Film formation; Spectroscopy

1. Introduction

There are few classes of polymeric materials which exhibit such unique and diverse property profiles as those achievable with polyurethanes (PURs). Even though research in the area of PURs has already spanned many decades, efforts to enhance knowledge pertaining to their structure-property relationships [1–3] continues due to the high performance characteristics of PURs in a wide variety of applications. One feature of PURs that is largely responsible for their favorable property profiles is the existence of heterogeneous, microphase separated domains, which may result from immiscibility of soft and hard blocks, [4–6] hydrogen bonding, [7–9] as well as chemically-induced separation of urethane-rich and urea-rich domains, [10,11] which has been directly observed using X-ray spectromicroscopy [12]. Furthermore, a number of studies have examined phase separation kinetics in PURs using spectroscopic approaches as well as thermal analysis [13–15].

Although the primary focus of previous efforts was on traditional solvent-based chemistries, a number of studies have focused on water-based urethane-containing colloidal systems. An obvious interest in water-based PURs stems from their low volatile organic content (VOC) levels. While attempts have been made to incorporate urethane functionalities into hybrid latex emulsions [16] or miniemulsions, [17] such approaches typically do not offer the performance of two-component (2K) solventborne PURs, which are thermosetting reactive systems comprised of multi-functional isocyanate-bearing crosslinkers mixed with oligomeric hydroxy-functional 'polyol' prepolymers in an organic solvent that crosslink upon application to a substrate. It is for this very reason that waterborne two-component polyurethanes (WB 2K-PURs) were introduced in the 1990's, which offer similar performance to 2K solventborne PURs, but with significantly reduced VOC.

The basic components of WB 2K-PUR systems typically include a hydroxy-functional water-reducible acrylic or polyester 'polyol' resin dispersion, an amine neutralizing

* Corresponding author. Tel.: +1 601 2666454; fax: +1 601 2665504.
E-mail address: marek.urban@usm.com (M.W. Urban).

0032-3861/$ - see front matter © 2005 Elsevier Ltd. All rights reserved.
doi:10.1016/j.polymer.2005.04.009

agent to facilitate aqueous dispersion of the polyol via neutralization of pendant carboxylic acid groups, an oligomeric polyisocyanate crosslinker derived from hexamethylene diisocyanate (HDI) or isophorone diisocyanate (IPDI) which may or may not be hydrophilically-modified, optional cosolvent(s), and water. Using appropriate shearing conditions, such components may be uniformly incorporated into a reactive colloidal dispersion having a desirable low viscosity (<100 mPa s), but with a limited useful application window often referred to as the 'pot life'. Unlike their solventborne counterparts, where progression of pot life may be visually assessed by observing the increase in viscosity, WB 2K-PUR reactive dispersions may not display significant changes in their rheological properties or appearance until the very end of the useful lifetime, at which time colloidal instability, sedimentation, gel formation, and foaming can be observed. Characterization of WB 2K-PURs in the aqueous state can also be quite elusive due to the complex, dynamic, and heterogeneous solution morphology of WB 2K-PURs.

Despite the practical knowledge regarding formulation and application of WB 2K-PURs that has been realized in the last decade, minimal scientific information exists pertaining to the fundamental processes occurring in the aqueous state or during film formation. While it is generally accepted that these systems are highly sensitive to a number of minute process and environmental variables, such as temperature, humidity, stoichiometric imbalance, pH, or shear history, to name a few, the precise roles of such variables prior to and/or during film formation have only recently begun to be addressed [18–27]. Since the dynamics of WB 2K-PURs in the aqueous state are likely to affect the final properties of resulting films, the objectives of these studies are to correlate solution morphological features with dynamics of colloidal processes in WB 2K-PUR reactive dispersions as well as to correlate solution morphological features with film morphology and film formation.

2. Experimental section

The materials utilized in these studies include a polyester 'polyol' aqueous dispersion and a water-dispersible polyisocyanate (WDPI); representative structures for each are shown in Fig. 1. The polyol resin utilized is a complex mixture of products, and the precise composition is unknown, although the resin may generally be considered as a copolyester of 1,3-benzenedicarboxylic acid (isopthalic acid, IPA), hexanedioic acid (adipic acid, AA), 2,2-dimethyl-1,3-propanediol (neopentyl glycol, NPG), and 2,2-dimethylolpropionic acid (DMPA). Such polyol was dispersed by mixing neat resin with a mixture of water and ammonium hydroxide, resulting in an approx. 30 wt% aqueous dispersion having a pH of approx. 8.0. Polyurethane/urea films were prepared by mixing polyol resin aqueous dispersion with neat Bayhydur 302 WDPI crosslinker using overhead agitation at 1800 rpm with a miniature 4-blade PTFE impeller in 20 ml glass vials. WDPI crosslinkers used in these studies contain approx 35 wt% poly(ethylene glycol), as determined by ^{1}H NMR. The relative amounts of each reactive component and water were adjusted to provide isocyanate to hydroxyl (NCO:OH) molar equivalent ratios ranging from 1.0 to 2.2. Total reactant concentrations were varied from 35 to 45 wt%. Following the mixing process, unless otherwise indicated, the reactive mixture was held without agitation for 10 min to allow for viscosity reduction and uniform film application, and such mixture was applied to obtain approx. 40 μm (+/−3 μm) thick dry films on glass slides which were crosslinked for 3 days in controlled environment chambers at 30 °C having 75 and 82% relative humidities (%RH).

Contact mode atomic force microscopic (AFM) images were obtained using a TA Instruments micro thermal analyzer 2990 which incorporates a Thermo Microscopes Explorer model AFM. Topographic images were acquired using scan rates ranging from 50 to 200 μm/s using a silicon nitride contact AFM probe. Transmission electron micrographs (TEM) were acquired on a Zeiss EM 109T microscope using an accelerating voltage of 80 kV. Samples of reactive dispersion used for TEM analysis were prepared by making a 1:10,000 dilution in deionized water followed by casting onto Formvar coated copper grids (Ted Pella, Inc.). No staining agents were used.

Particle size distribution (PSD) measurements were performed on a Nanotrac dynamic light scattering particle size analyzer, Model NPA250 (Microtrac Inc.) equipped with a fiber optic probe assembly. Samples for PSD analysis were prepared by diluting one drop of dispersion in approx. 15.0 ml of DI water with gentle swirling. Measurements were performed at ambient temperature (approx. 22 °C) and were sensitive to particle diameters in a size range of 3–6 μm. Reported mean particle size values represent the mean particle diameter as calculated from the volume distribution (MV).

Solution ^{1}H nuclear magnetic resonance (NMR) spectroscopic measurements were performed on a Varian INOVA spectrometer operating at 500 MHz. Aqueous samples of admixed WB 2K-PUR reactive dispersions were run after 10 min of mixing in unlocked mode without using deuterated solvents, as described by Hoye et al. [28]. Relative chemical shifts were assigned relative to the water resonance (4.80 ppm relative to TMS). A presaturation pulse sequence (1.5 s presaturation delay) was implemented to suppress the resonance from water, due to the high concentration of water in the admixed dispersions. A 90° pulse angle was employed (12.6 μs pulse width) with a 3 s recycle delay. In situ reaction kinetic measurements were made by acquiring spectra every 10 min over the time period of 10–150 min from the time WDPI was first added to the polyol/water mixture using 64 transients per measurement. Spin–spin relaxation times (T_2) of reactive

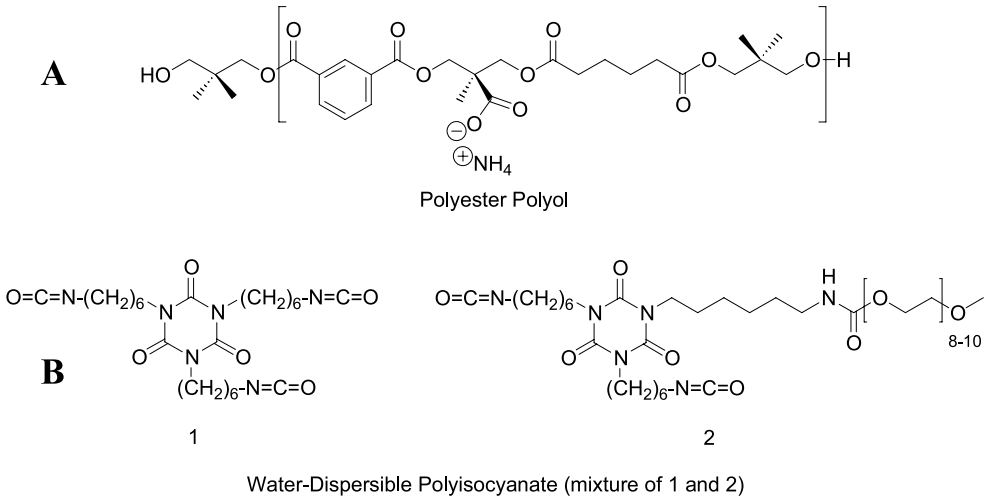

Fig. 1. Representative structures for WB 2K-PUR materials used in these studies.

dispersions were determined using a Carr–Purcell–Meiboom–Gill pulse sequence [29,30] with preceeding presaturation (i.e. presat$-\pi/2-(\tau-\pi-\tau)_n-$Acq) using a recycle delay of 1.0 s, a presaturation delay of 1.5 s, an echo time, τ, of 4.0 ms, an acquisition time of 1.5 s, and an array of 13 values for the echo number, n. Four transients per array increment were acquired, resulting in a time of 187 s per arrayed data set. Measurements were made every 5 min, and T_2 values were calculated using a least squares fitting algorithm provided with Varian VNMR 6.1c software.

3. Results

Fig. 1 depicts representative structures of polyol and polyisocyanate oligomers comprising the 2K system. Neutralized pendant ammonium carboxylate groups are attached to the polyol backbone, which is accomplished by incorporation of 2,2-dimethyolpropionic acid (DMPA), followed by subsequent neutralization with ammonia. Amine salts can impart significant hydrophilicity to polyol chains such that, upon partial neutralization to slightly basic conditions (pH = 7–8), fine aqueous polyol dispersions may be achieved in which surface-bound ammonium carboxylate groups stabilize spherical particles via electrostatic repulsion. As shown in Fig. 2A, dilute polyol dispersion particle size distributions (PSD) are narrow and unimodal with a mean diameter of 18 nm ($\sigma = 5$ nm). Polyisocyanate crosslinker has no ionic content to impart water-dispersibility, but instead, a fraction of the isocyanate groups may be reacted with short mono-functional poly(ethylene glycol) segments, which function as internal, non-ionic surfactants. This results in a mixture of unmodified and PEG-modified NCO-functional crosslinkers, as shown in Fig. 1A and B. Upon using appropriate shearing conditions, such water-dispersible polyisocyanates (WDPI) are capable of forming fine aqueous dispersions, where PEG-modified crosslinkers are presumed to be located around the periphery of droplets containing unmodified crosslinker. As shown in Fig. 2B, the mean particle diameter of WDPI aqueous dispersion is 90 nm ($\sigma = 37$ nm), however, upon mixing undiluted WDPI into diluted aqueous polyol dispersion at 1800 rpm for 10 min, the resulting PSD has an initial mean diameter of 150 nm ($\sigma = 43$ nm). This is shown in Fig. 2, trace C. Although the particle size increase is quite surprising, no bimodality is detected under these conditions, which indicates that little, if any, polyol exists as a freely, unassociated polyol droplet. The same applies to WDPI. Consequently, the individual components of the WB 2K-PUR reactive dispersion are likely in close spatial proximity to each other, although at this point the microstructural nature of the reactive dispersion is not understood.

In an effort to determine which process parameters have a significant effect on the colloidal state of WB 2K-PUR reactive dispersions, PSD data was acquired as a function of total reactant concentration (35–45 wt%), while maintaining a consistent reactant stoichiometry of NCO:OH = 2.0 at 25 °C. These data are shown in Fig. 3A, and as seen, average particle diameters are approx. 150 nm ($\pm$10 nm) for all reactant concentrations at 10 min. However, at extended times, the average particle diameters for all concentrations increase, but the rate of increase is concentration dependent. Specifically, 45 wt% total reactant concentration results in the most rapid increase of average particle diameter, with particle diameters of approx 500 nm at 110 min, whereas the 35 wt% reactive dispersion attained a maximum avg. particle diameter of approx. 180 nm at 120 min. For comparison, a 45 wt% aqueous dispersion of only WDPI is also shown in Fig. 3, and as seen, the average particle size essentially remains constant at approx. 120 nm for the 2 h duration of the experiment. Consequently, the presence of polyol is necessary for the observation of an increase in particle size over time. These observations raise two important questions; namely, what is the mechanism for

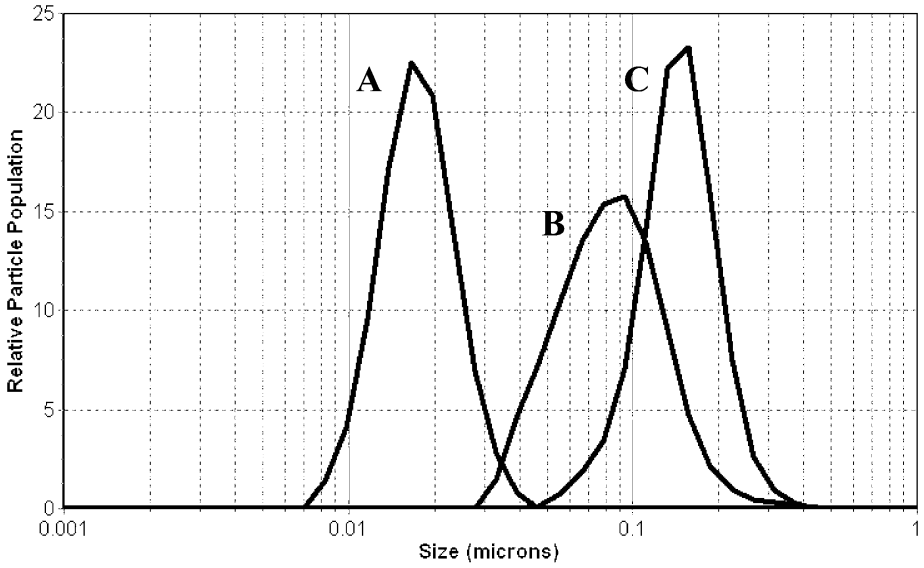

Fig. 2. Particle size distributions of A. polyol, B. polyisocyanate, and C. reactive colloidal dispersion of A and B with NCO:OH = 2.0 after 10 min of mixing at 1800 rpm and 25 °C.

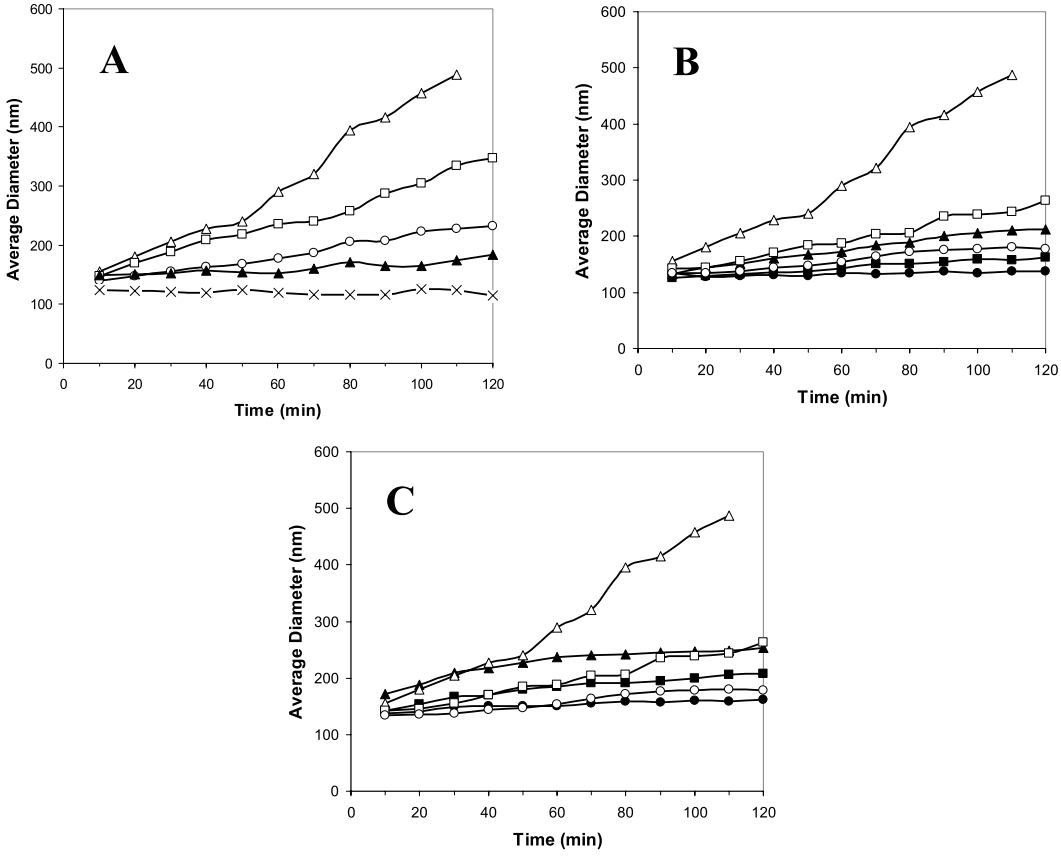

Fig. 3. Particle size data for WB 2K-PUR reactive dispersions: A. Effect of overall reactant concentration on time evolution of average particle size in WB 2K-PUR reactive dispersions. NCO:OH = 2.0, mixed at 1800 rpm for 10 min. Reactant concentrations: △, 45%; □, 43%; ○, 40%; ▲, 35%; ×, 45% (WDPI only). B. Effects of temperature and NCO:OH ratio on time evolution of average particle size in WB 2K-PUR reactive dispersions. 20 °C NCO:OH ratios: ●, 1.0; ■, 1.5; ▲, 2.0. 25 °C NCO:OH ratios: ○, 1.0; □, 1.5; △, 2.0. C. Effect of mixing duration on time evolution of average particle size in WB 2K-PUR reactive dispersions. 45 wt% total reactant concentration, 25 °C. Continuously mixed, NCO:OH ratios: ●, 1.0; ■, 1.5; ▲, 2.0. Mixed for 10 min, NCO:OH ratios: ○, 1.0; □, 1.5; △, 2.0.

rapid increase in particle diameter in WB 2K-PUR reactive dispersions, and what variables affect this process?

In an effort to address these questions, Fig. 3B shows average particle size increases as a function of temperature (20 and 25 °C) as well as reactant stoichiometry (NCO:OH = 1.0, 1.5, 2.0), while maintaining a consistent total reactant concentration of 45 wt%. Again, the initial average particle sizes at 10 min for all conditions are similar, and are approx. 135 (±10 nm). However, increased reactant stoichiometry and increased temperature result in faster rates of particle size increase. Attempts to monitor particle size increases at 30 °C failed as a result of premature gellation at approx. 30–50 min, implying a very rapid rate of particle size increase.

Let us now focus on the effect of shear time on particle size. To this point, all data shown in Fig. 3A and B were obtained from reactive dispersions that were mixed for an initial 10 min, and were then held without agitation for the remainder of the experiment. Fig. 3C compares such mixing conditions at 45 wt% reactant concentrations and 25 °C for various reactant stoichiometries along with identical specimens that were mixed for the entire duration of the experiment (2 h). As seen, for all reactant stoichiometries, both mixing conditions result in similar increases of the initial average particle size, but continuously mixed dispersions do not attain as high of an average particle size as their 'resting' counterparts. This difference is most pronounced at an NCO:OH ratio of 2.0 in which the particle size begins to diverge at approx. 40 min, and at 110 min, continuously mixed dispersion has a particle size of approx. 250 nm, whereas the dispersion mixed for 10 min exhibited particle size of nearly 500 nm. While previous studies [31,32] have speculated that extended or excessive shears could have an adverse affect on the stability of WB 2K-PUR reactive dispersions, our data clearly indicate that extended shearing serves to retard the increase in particle size over time, which ultimately increases the colloidal stability of the dispersion.

During the course of these studies it was also observed that films prepared using different mixing times exhibited different surface topographical properties when crosslinked at elevated relative humidities (RH). To illustrate this effect, topographic AFM images were collected, and representative examples are shown in Fig. 4, which illustrate a progression of AFM images from PUR films sheared for 10 (A), 30 (B), and 50 (C) min at 1800 rpm with an NCO:OH ratio of 2.2. These films were crosslinked at 75%RH and 30 °C for 3 days. As seen in Fig. 4, image A, after 10 min of mixing, significantly larger, less uniform surface features are detected. In contrast, images B and C, representing longer mixing times, respectively, do not exhibit these features. A similar effect is detected for films crosslinked at 82%RH and 30 °C, which are depicted in Fig. 4, images D–F. In these experiments, WB 2K-PUR dispersions were sheared for 10, 60, and 120 min, respectively. It should be noted that the magnitude of the features is significantly larger for these conditions. Specifically, the topographical features of these images are on the order of 300 nm in the z-direction, and a larger x–y scale of 100 μm is used. In view of the above observations, it is reasonable to suspect that dynamic processes occur early in the lifetime of the WB 2K-PUR reactive dispersions that have a profound latent effect on the surface topography of resulting films.

While a number of studies have focused on the NMR analysis of polyurethanes and their starting materials, [33–35] very few NMR experiments have specifically dealt with waterborne polyurethanes, [36] and there are good reasons for that. WB 2K-PUR dispersions are formulated without the use of organic solvents. Since water is used as a dispersing medium, the choice of an NMR solvent is limited to water or deuterium oxide. As a matter of fact, the use of any organic solvent would not be desirable, as it will alter the inherent WB 2K-PUR solution morphology. Furthermore, since the dispersed reactants are highly concentrated, reduced segmental mobility can lead to line broadening, thereby limiting resolution of individual resonances. Finally, the concentration of water in WB 2K-PUR reactive dispersions is at least 50% w/w, and suitable measures must be taken to suppress the water resonance in the NMR spectra.

With these considerations in mind, Fig. 5, traces A–C, illustrate ^{1}H NMR spectra of WDPI aqueous dispersion, polyol aqueous dispersion, and WB 2K-PUR reactive dispersion, respectively, obtained using the pulse sequence outlined in Section 2. As seen, all spectra display well-resolved features characteristic of functional groups contained in each component. While a rigorous interpretation of all resolvable resonances observed in these spectra is not the primary focus of the current studies, assignments are limited to peaks relevant to solution morphological features. As shown in Fig. 5, trace A, the linewidths are somewhat broadened, which is likely attributed to the presence of dispersed colloidal droplets containing non-solvated, oligomeric crosslinker. The neat viscosity of WDPI ranges from 2000 to 4000 mPa s, which implies significantly retarded mobility as well as relatively short spin-spin relaxation times (T_2), and broad peaks centered at 1.42 and 1.67 ppm result from overlapping sets of aliphatic methylenes at positions 3 (γ) and 2 (β), respectively, due to either end of the hexamethylene chains of WDPI crosslinkers. The NCO α-methylene resonance appears at 3.36 ppm, and the isocyanurate α-methylene resonance is detected as a shoulder at approx. 3.65 ppm on the peak at 3.71 ppm due to PEG –(CH_2–CH_2–O)– protons [37,38]. A comparison of resonances in Fig. 5, trace B, due to aqueous polyol dispersion, with WDPI dispersion (trace A) indicates narrower linewidths in trace B, which is attributed to the relatively high mobility of polyol in slightly basic aqueous media. This observation also indicates that polyol aggregates are, to some degree, water-swollen at a pH of 7.8. Since NMR spectra of polyol aqueous dispersions neutralized with additional ammonia to a pH of 9.8 (not shown)

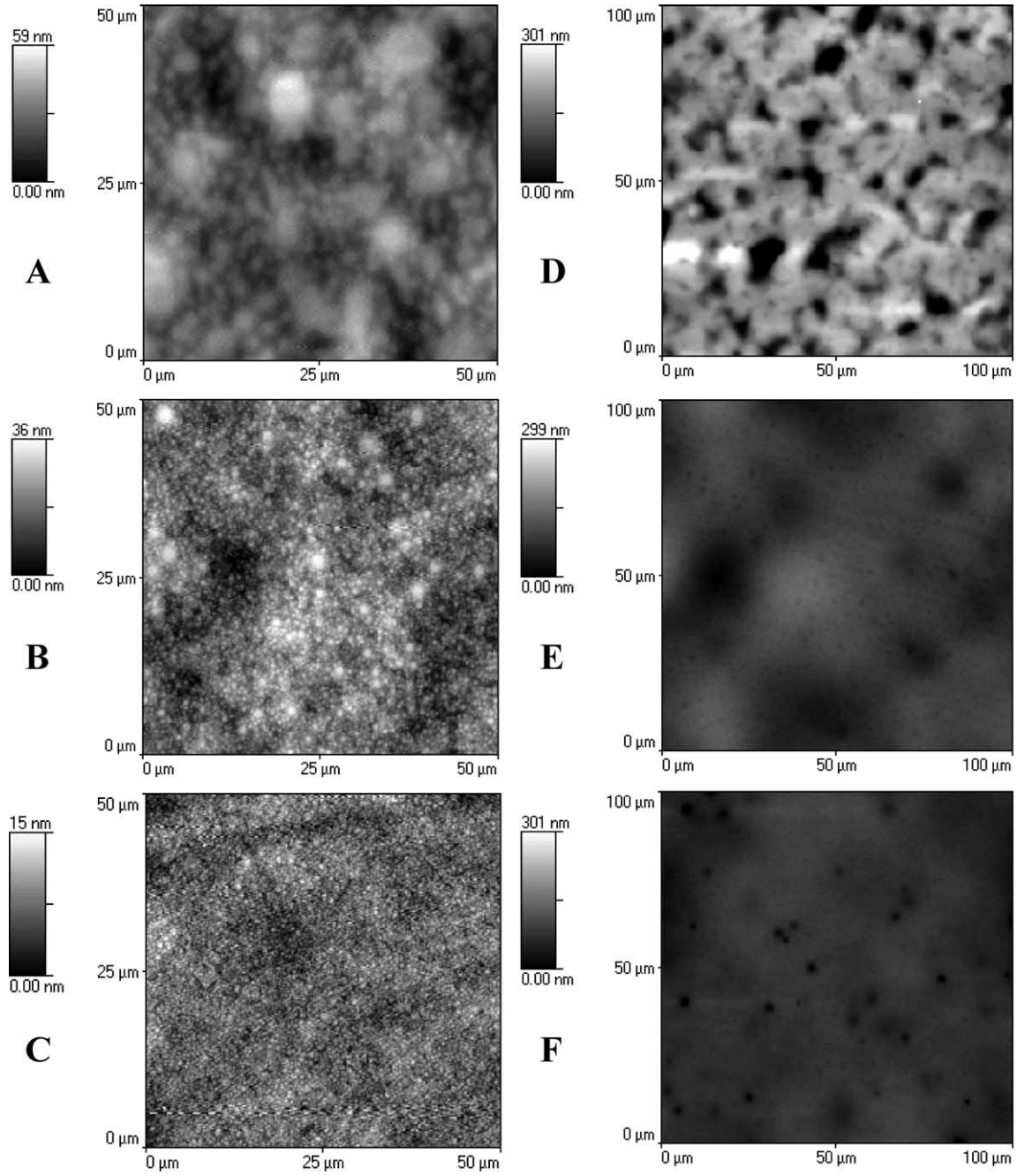

Fig. 4. Topographic AFM images of PUR films after mixing at 1800 rpm prior to film application. Mixing times (min) for films crosslinked at 75%RH and 30 °C; A. 10, B. 30, C. 50. Mixing times (min) for films crosslinked at 82%RH and 30 °C; D. 10, E. 60, F. 120.

displayed even narrower linewidths with more resolved multiplicities than the spectrum shown in Fig. 5B, the pH of the polyol aqueous dispersion strongly affects the mobility of the polyol as well as the T_2 relaxation times. Pertinent chemical shifts of Fig. 5, trace B include 1.58 ppm (adipic acid/adipate ester overlapping β-methylenes), 2.16 ppm (adipic acid end group α-methylenes), and 2.38 ppm (adipate ester α-methylenes) [36]. While Fig. 5, trace C (WB 2K-PUR reactive dispersion) clearly displays resonances arising from the combination of the individual components, the most pertinent feature of this spectrum is the broad, intense peak at 3.63 ppm primarily due to PEG protons with a sharp shoulder at approx. 3.61 ppm, likely due to NPG or DMPA hydroxyl α-methylenes. It should be noted that the intensity of the resonance at 3.63 ppm increases over time relative to the other peaks in the spectrum during kinetic investigations of the WB 2K-PUR reactive dispersion.

In an effort to determine why the PEG resonance in Fig. 5, trace C increases with time in WB 2K-PUR reactive dispersions, the temporal behavior of the PEG resonance (3.73 ppm) in WDPI aqueous dispersions was investigated.

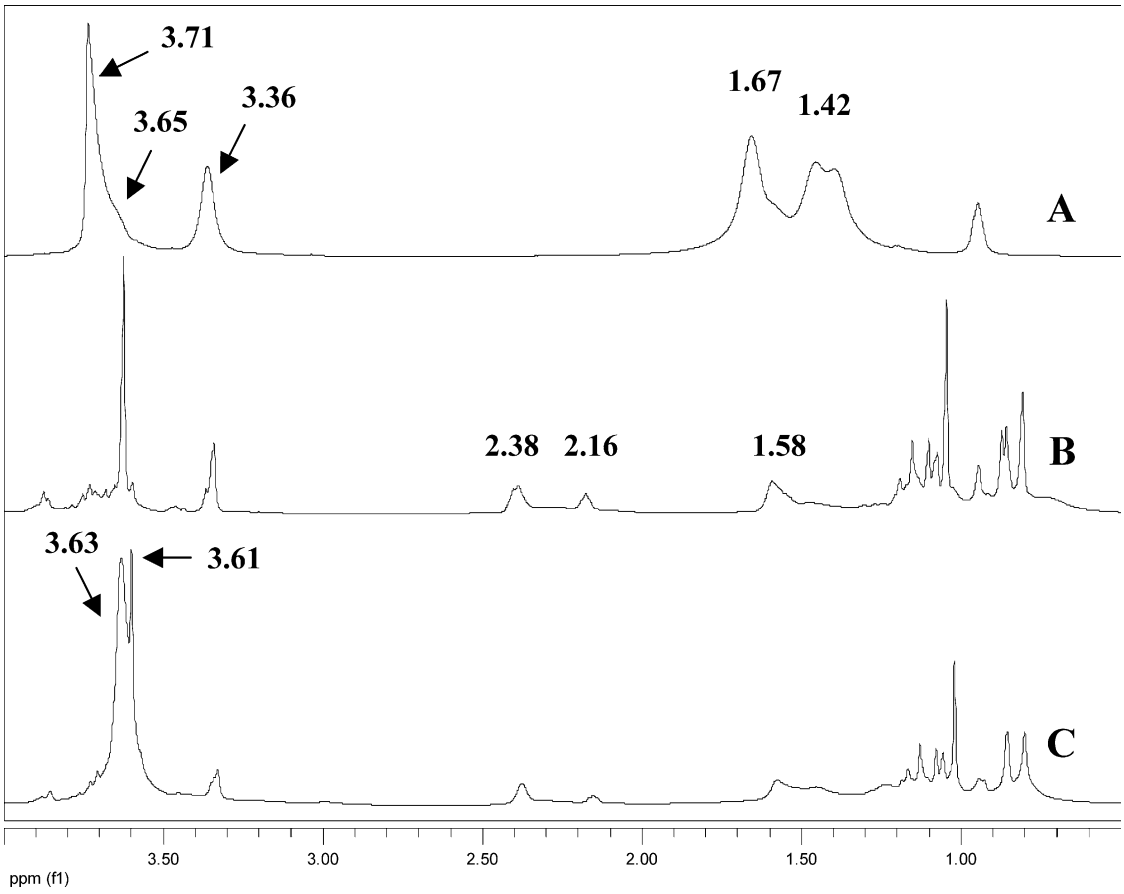

Fig. 5. 500 MHz ^{1}H NMR spectra of aqueous materials used in these studies. A. Water-dispersible polyisocyanate emulsion, 25.0 wt% in water 35 min after preparation. B. Polyol aqueous dispersion, 28.8 wt% in water, pH = 7.8. C. WB 2K-PUR reactive dispersion, NCO:OH = 2.0, 30 min after preparation.

As illustrated by Fig. 6, enlarged traces A and B, which correspond to 45 and 155 min in the aqueous colloidal state, respectively, the PEG resonance increases relative to all other aliphatic resonances. Furthermore, line-narrowing of the PEG resonance due to a mobility increase is observed, which likely results from progressive hydration of PEG chains inside the core of WDPI droplets, as the local environment surrounding occluded PEG moieties changes from one rich in isocyanurate-based crosslinker to one richer in water, although the mechanism of PEG hydration is not obvious. Finally, the remaining aliphatic peaks in Fig. 6, traces A and B, overlap, indicating no change in linewidth, thereby indicating minimal change in the mobility of hydrophobic WDPI entities within the timeframe of the experiment.

One of the main questions to be addressed regarding the WB 2K-PUR reactive dispersion is which chemical reactions take place during the pot life, and what are their effects on solution morphology? In order to address this question, Fig. 7 was constructed, which illustrates ^{1}H NMR spectra of WB 2K-PUR reactive dispersion at 15 (trace A) and 75 min (trace B), respectively, after preparation. By comparison of the two spectra, a number of changes in resonance intensities are observed, but of particular interest are the peaks at 6.80 and 6.25 ppm, which correspond to N–H protons of urea and urethane functional groups, respectively. Since no previous NMR studies of waterborne polyurethanes in an aqueous environment have been reported, we make these assignments based on the fact that the 6.80 ppm resonance due to urea was also detected in spectra of aqueous dispersions of WDPI (not shown) after 155 min, but not at 45 min. Since no polyol was present in the WDPI dispersion, it is reasonable to assume that urea forms as a result of NCO reactions with H_2O. Furthermore, previous NMR studies of other polyurethane precursors have indicated that the urea N–H peak exists at higher magnetic field than urethane N–H peaks [36]. In addition, the intensities of the urethane and urea N–H peaks appear to be very low, and the T_1 relaxation time of N–H protons can be significantly higher than C–H protons when proton exchange is slow. Finally, the multiplet at approx. 7.50–7.65 ppm corresponds to the aromatic C–H moieties of isopthalate repeat units of the polyol that are meta-substituted, relative to both ester groups, and do not correspond to urethane or urea reaction products.

In an effort to quantitatively assess the mobility of individual moieties in WB 2K-PUR reactive dispersions, spin–spin (T_2) relaxation times were measured over the

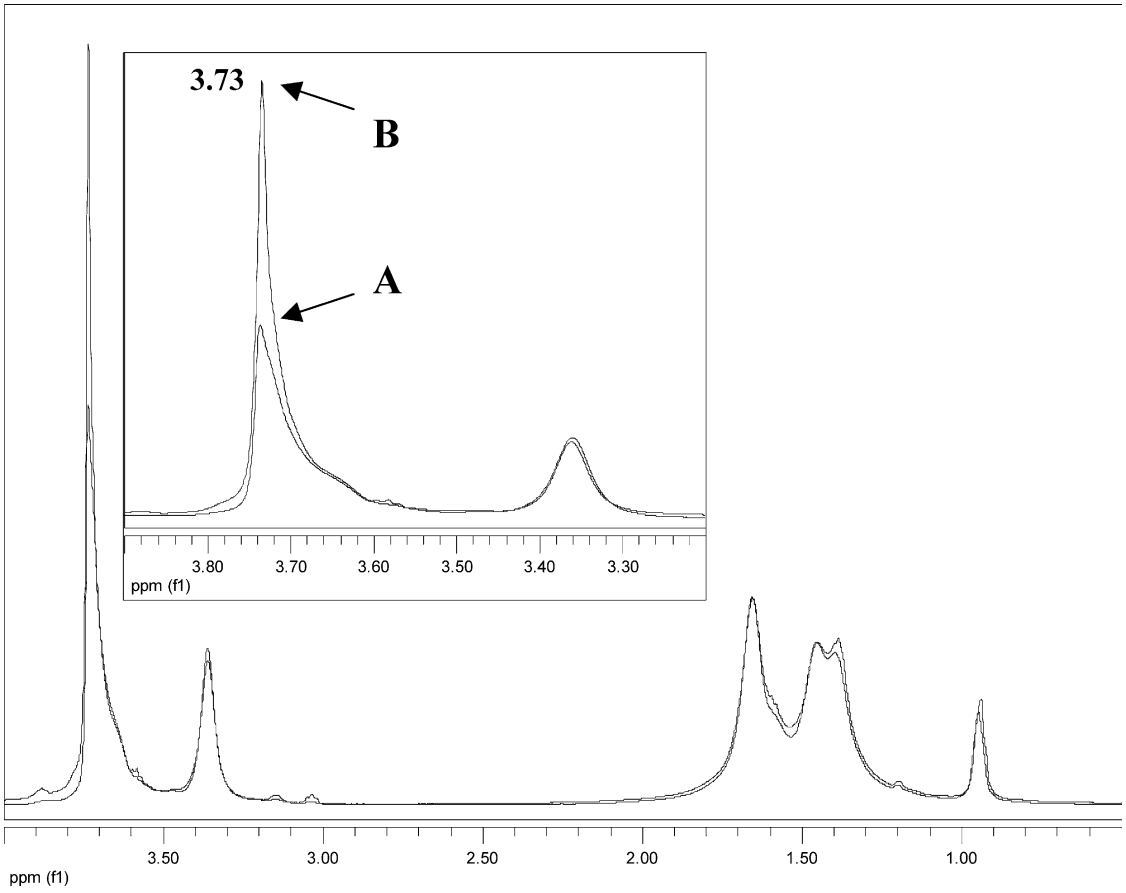

Fig. 6. 500 MHz ^{1}H NMR spectra of water-dispersible polyisocyanate emulsion, 25.0 wt% in water. A. Spectrum taken at 45 min. B. Spectrum taken at 155 min. Inset illustrates line-narrowing of PEG –(CH_2–CH_2–O)– protons with increasing time.

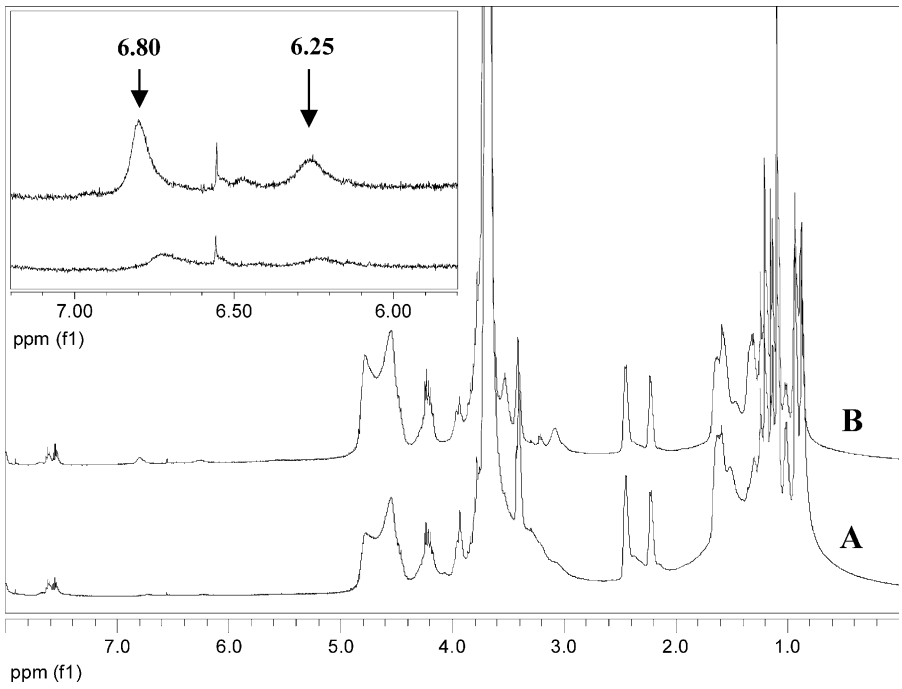

Fig. 7. 500 MHz ^{1}H NMR spectra of WB 2K-PUR reactive dispersion, 45.0 wt% in water. A. Spectrum taken at 15 min. B. Spectrum taken at 75 min. Enlarged inset illustrates N–H protons associated with urea (6.80 ppm) and urethane (6.25 ppm) formation in the aqueous, colloidal state.

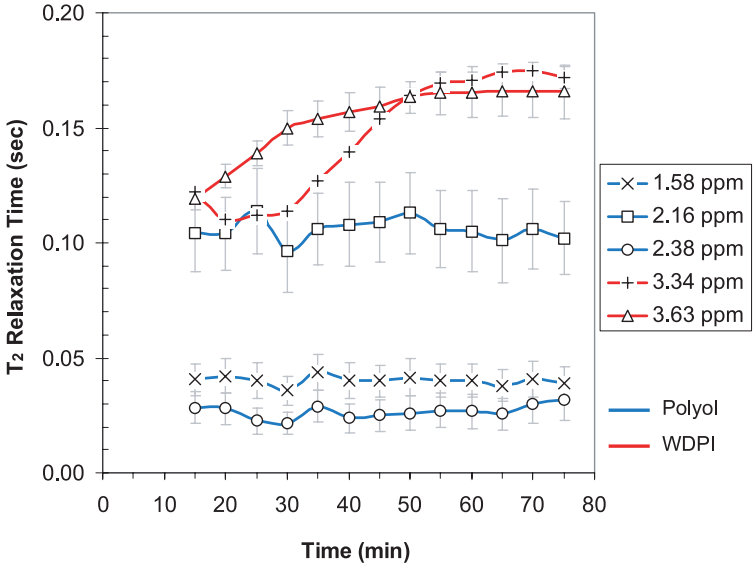

Fig. 8. Spin–spin relaxation times (T_2) for various resonances of WB 2K-PUR reactive dispersions as a function time from the start of mixing.

lifetime of the dispersions, and the plot of T_2 values as a function of time is depicted in Fig. 8. As seen, resonances at 1.58, 2.16, and 2.38, associated with polyol, have T_2 values that remain essentially constant within the experimental timeframe. On the other hand, the PEG resonance at 3.63 ppm sharply increases at the early stage, and then reaches a plateau at approx. 50 min. Furthermore, the resonance at 3.34 ppm (isocyanate α-methylene) also displays an increase in T_2, although the onset of the increase seems to be delayed somewhat (25–30 min), and also enters a plateau regime at approx. 50–60 min.

4. Discussion

As shown in Fig. 8, the polyol T_2 values remain unchanged indicating that the average degree of hydration of polyol remains constant within the first hour of the reactive dispersion's lifetime, and that little, if any, crosslinking occurs between polyol and polyisocyanate in the solution state. Furthermore, any pH change that may be occurring in the reactive dispersions that could potentially cause the polyol to collapse upon itself as a result of acidification of pendant carboxylate groups does not significantly affect the average mobility of the polyol. Thus, the T_2 profile of the PEG protons is consistent with the data shown in Fig. 6; namely, the PEG protons are becoming more mobile as the degree of WDPI hydration increases, and a steady-state degree of hydration is achieved after about 60 min. Consequently, the increase in particle size of WB 2K-PUR reactive dispersions shown in Fig. 3 is likely related to water ingress into the WDPI droplets.

In an effort to gain further insight as to the relationship between the observed T_2 values and the local environment surrounding PEG chains, spin–spin relaxation times for a series of PEG-containing samples were measured and are listed in Table 1. The PEG chains in undiluted PEG-modified WDPI display the shortest T_2 times (12.3 ms), which is attributed to the oligomeric, viscous nature of the non-solvated material. This is schematically depicted in Fig. 9A, which shows that in this environment, PEG chains are in close proximity to aliphatic hexamethylene chains, isocyanate, and isocyanurate moieties of WDPI components. However, T_2 times are significantly lengthened (120–240 ms) when WDPI is dispersed in water, which is shown in Fig. 9B. In this case, T_2 values increase with time, as was previously discussed in Figs. 6 and 7. The T_2 increase is attributed to the fact that a significant fraction of the PEG chains are initially in a solvated state at the periphery of WDPI droplets. However, the balance of the PEG chains remain buried within the core of the WDPI droplet at early times, but later become hydrated as water ingresses into WDPI droplets. Consequently, the observed T_2 values represent a weighted average of T_2 times associated with surface-bound, hydrated PEG chains and

Table 1
Spin–spin (T_2) relaxation times for –(CH_2CH_2O)– polyether resonances of components used in WB 2K-PUR reactive dispersions

Material	wt%	wt% H_2O	T_2 (ms)	Calculated error (ms)
Water-dispersible polyisocyanate	100	n/a	12.3	4
Water-dispersible polyisocyanate	25	75	120–240	11
WB 2K-PUR reactive dispersion	45	55	120–165	8
Poly(ethylene glycol), M_n=600	100	n/a	168	18
Poly(ethylene glycol), M_n=600	25	75	800	120

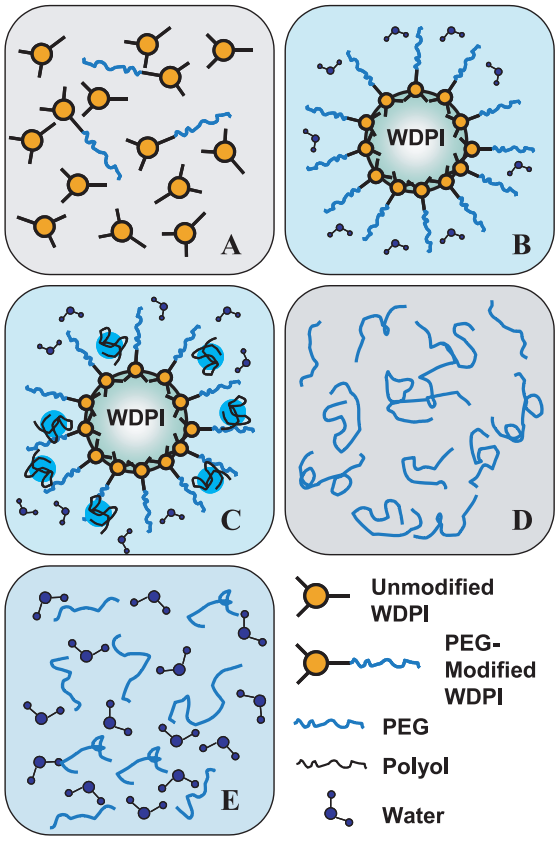

Fig. 9. Schematic illustration of localized environments surrounding poly(ethylene glycol) (PEG) segments for samples studied by ^{1}H NMR in these studies. A. WDPI; B. WDPI aqueous dispersion; C. WB 2K-PUR reactive dispersion; D. PEG; E. PEG aqueous solution.

core-localized PEG chains that are initially not hydrated, but become hydrated over time.

A similar behavior is observed for WB 2K-PUR reactive dispersions, which is schematically depicted in Fig. 9C. The T_2 values are initially approx. 120 ms, but gradually increase to approx 165 ms, as seen in Fig. 8. A comparison of maximum T_2 values of WB 2K-PUR reactive dispersion with their WDPI aqueous dispersion counterparts reveals a significant difference. WDPI aqueous dispersion reaches a maximum value of approx. 240 ms, whereas the WB 2K-PUR reactive dispersion only reaches a value of 165 ms. This behavior is likely attributed to the fact that in the WB 2K-PUR reactive dispersion polyol particles near the periphery of the WDPI droplets may constrain the mobility of surface-bound PEG chains as well as slow down the rate of water diffusion into WDPI droplets. Furthermore, crosslinking reactions between polyol and WDPI near the periphery of WDPI droplets could also effectively result in a partially crosslinked boundary layer.

Further analysis of the T_2 values for polydisperse PEG (M_n = 600 g/mol) and a 25 wt% aqueous solution thereof indicates that unsolvated PEG T_2 values are similar to WDPI aqueous dispersion as well as WB 2K-PUR reactive dispersion. In contrast, for PEG aqueous solutions, which is schematically depicted in Fig. 9E, the longest measured T_2 times of approx 800 ms are detected, indicating the highest mobility environment. Consequently, the PEG chains in both WDPI and WB 2K-PUR dispersions exhibit constrained mobility, relative to aqueous PEG solutions, which is attributed to the local environment of covalently attached PEG chains on crosslinkers and the closely packed geometry of PEG chains around the periphery of the WDPI droplet.

Up to this point we have utilized the T_2 values to determine mobility of individual components in their reaction environments and concluded that water ingresses into WDPI droplets and hydrates core-localized PEG-modified crosslinkers. However, the presence of water in the WB 2K-PUR reactive dispersion may also result in reactions with isocyanate groups to form urea linkages (crosslinks), as shown in Fig. 7, and carbon dioxide [39]. It is this side reaction that was originally the main obstacle associated with the development of WB 2K-PUR materials, limiting crosslinking with polyols and leading to CO_2 formation in PUR films. Although addition of a stoichiometric excess of polyisocyanate crosslinker compensates for the sacrificial reactions of isocyanate groups with water, we take advantage of these reactions and illustrate how typically undesirable side reactions may actually benefit reacting NCO and OH functionalities in an aqueous environment and lead to more homogeneous films.

As previously indicated, the presence of polyol is necessary to observe an increase in the average particle size with time for aqueous dispersions containing WDPI (Fig. 3A–C). However, WDPI aqueous dispersions retain their particle size of approx. 120 nm for over 2 h after formation of the respective aqueous dispersion. Aqueous polyol dispersions are also stable and exhibit good stability (months), with particle sizes of approx. 18 nm, depending on the pH of the aqueous dispersion, typically 7–8 pH units. However, below this range, an insufficient fraction of DMPA acid groups are neutralized to provide sufficient hydrophilicity to polyol chains or enough electrostatic repulsions to stabilize droplets, making the polyol effectively non-dispersible. Above that pH, polyol droplets become smaller (<15 nm) and more hydrophilic, but as a result of water swelling, the solution viscosity of polyol dispersions at pH>9 increases due to chain entanglements. Given sufficient time, the nearly molecularly solvated polyol chains begin to self-associate and further entangle, resulting in formation of a gel which precipitates out of solution. Thus, the solution stability of colloidal polyol aggregates is strongly dependent upon the pH. However, if polyol particle collapse is indeed responsible for WB 2K-PUR reactive dispersion destabilization, the question is what mechanisms are responsible for this behavior?

In an effort to address this question, and considering the data discussed in Figs. 1–7, we recorded TEM micrographs which are shown in Fig. 10A and B. These images were obtained from WB 2K-PUR reactive dispersions after 1 h of

mixing (NCO:OH = 1.5). As shown in Fig. 10A, an aggregate of six WDPI droplets is observed in which their original spherical particle morphology is evident, although the reason for aggregation is not. If the interstitial regions between individual WDPI particles contain destabilized polyol, cohesion of WDPI particles could result. Further analysis of this figure shows that a few small particles are visible on the right side of the aggregate, and their sizes are consistent with adsorbed polyol droplets, referring back to Fig. 2A. These aggregates are found throughout the entire WB 2K-PUR TEM specimen, which are shown in Fig. 11B. Thus, the formation of aggregates is related to the increase in particle size observed in Fig. 3, and the inset of Fig. 10B also illustrates aggregated WDPI spheres with surface-bound polyol adsorbates.

In an effort to explain how morphological features detected in TEM micrographs shown in Fig. 10 are formed, the model illustrated in Fig. 11 is proposed. In part A of this figure, initially, a large WDPI droplet with an ammonium carboxylate stabilized polyol droplet are shown, along with ammonia and water. As seen, the WDPI droplet surface is stabilized by hydrophilically-modified crosslinkers, although a significant fraction of these may be found within the core of the WDPI droplet, along with unmodified crosslinkers. While a significant fraction of ammonia neutralizes pendant acid groups of polyol, ammonia is also free to diffuse into the WDPI droplet, as indicated by Scheme A1. In such a scenario, ammonia reacts with NCO groups to first form a primary urea, which is then capable of reacting with another NCO group to form polyurea (PUA), which was observed by NMR in Fig. 7. Scheme A2 illustrates how water can also ingress into the WDPI droplet over time, thereby allowing the core-localized PEG segments of hydrophilically-modified crosslinkers to become hydrated, and more mobile, which accounts for the observed increased T_2 values in Figs. 6, 8, and 9 that was previously discussed. At the same time, water within the WDPI droplets is capable of reacting with NCO groups, leading to an unstable carbamic acid intermediate, which decomposes to a primary amine and CO_2. While the primary amine will undoubtedly quickly react with another NCO group to form PUA, the fate of the CO_2 is more complex. CO_2 is known to dissolve in water (approx. 1.8 g/l^{-1}at 20 °C), and about 1% of the dissolved carbon dioxide can then react with water to form carbonic acid, [40] as shown in Fig. 11, Scheme A3. Since the WB 2K-PUR system is a buffered, slightly basic system, any carbonic acid that is formed will compete with the pendant carboxylate groups of polyol chains for available ammonium ions, thereby destabilizing the dispersed polyol droplets by reducing their extent of neutralization. In the same manner, any consumption of ammonia by NCO groups, as illustrated in Scheme A1, can further destabilize polyol droplets by reducing the amount of available neutralizing agents.

Upon destabilization of polyol by effective removal of available neutralizing species, the degree of water swelling decreases, and the polyol droplets collapse. Such a process may be enhanced by intramolecular hydrogen bonding of pendant acid groups, facilitating its collapse and subsequent adsorption to the WDPI droplet surface. When such a process occurs repeatedly over time, the surface of WDPI droplets would become speckled with small acidified polyol

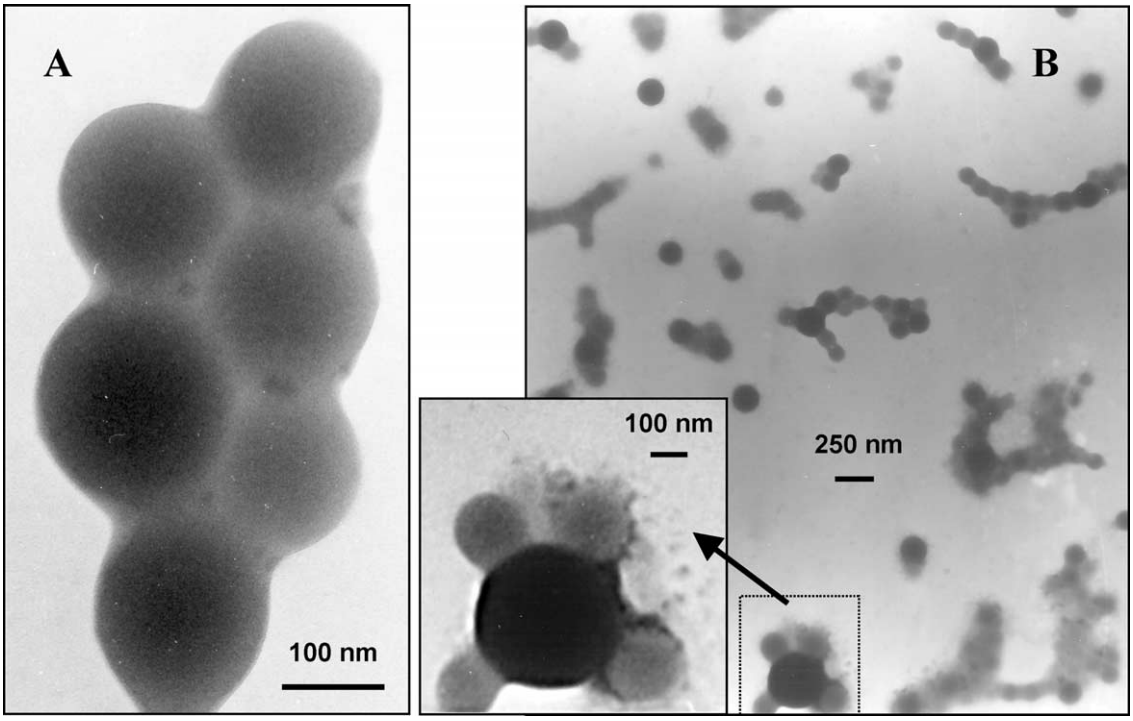

Fig. 10. TEM images of aggregates formed in WB 2K-PUR reactive dispersions at 60 min NCO:OH = 1.5, 45% solids, 25 °C.

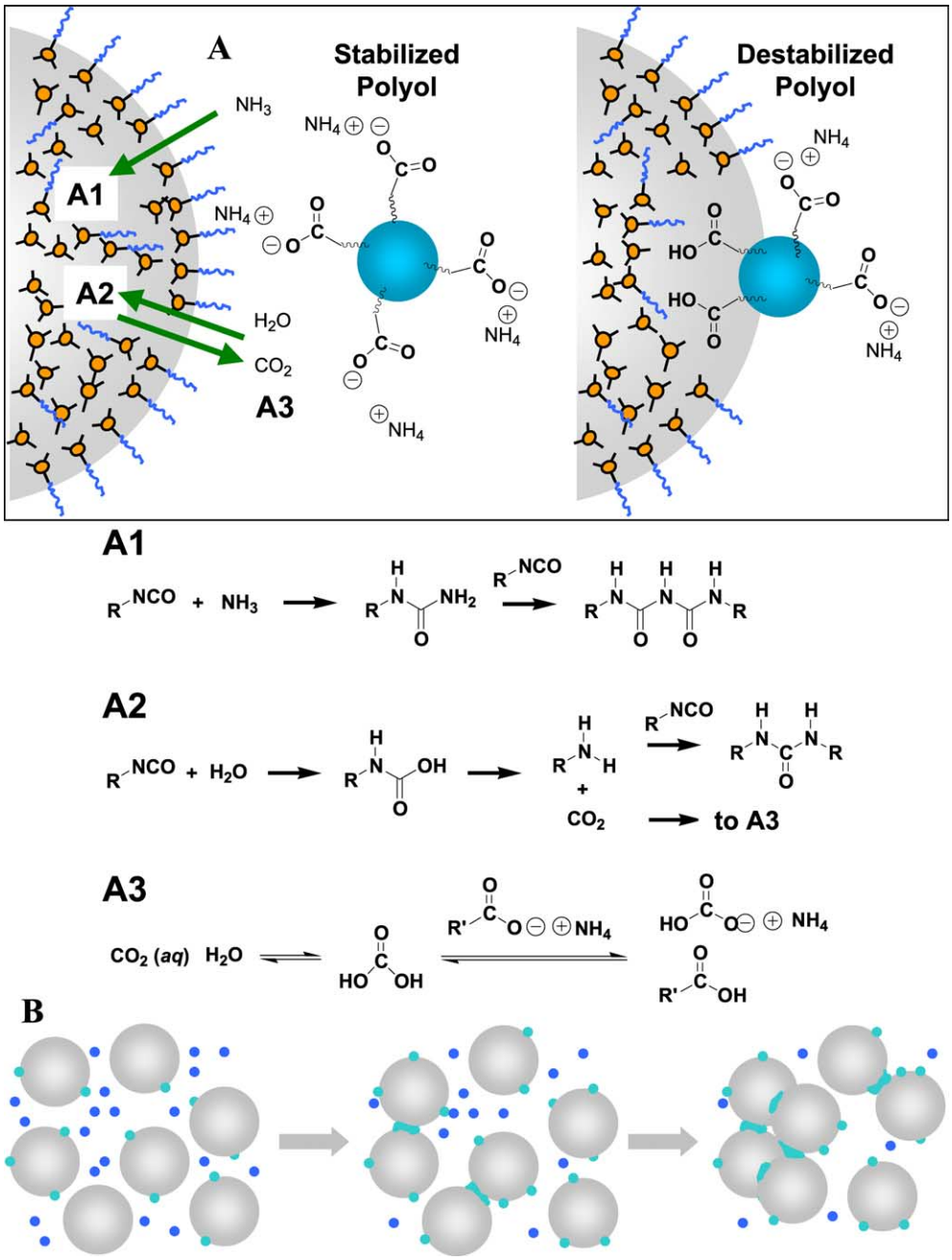

Fig. 11. A. Schematic illustration of polyol destabilization and subsequent adsorption to WDPI surface with corresponding reactions. B. Clustering of WDPI droplets with adsorbed polyol to form aggregates.

adsorbates having adhesive properties. With time, these polyol adsorbates will cohere between individual WDPI droplets followed by subsequent formation of aggregates. This is schematically illustrated in Fig. 11B.

The model proposed depicted in Fig. 11A and B would result in an increase in the average particle size of the reactive dispersion via aggregate formation, which was observed and discussed in Figs. 3 and 10. A number of variables such as concentration of reactants and reactant stoichiometry should also affect the rate at which such an aggregation process occurs, which again was observed in Fig. 3A, where increasing concentrations of reactants accelerate the rate of aggregation with the process being attributed to increased frequency of collisions between individual WDPI droplets with adsorbed polyol. Furthermore, as the stoichiometric excess of isocyanate is increased, there are more WDPI droplets in solution and thus greater surface area of WDPI droplets is available. Therefore, higher NCO:OH ratios will result in faster rates of aggregation, as observed in Fig. 3B. Additionally, the mechanical forces imposed by shearing conditions in the aqueous dispersion can reverse the aggregation process, as

was illustrated in Fig. 3C which showed that continuous mixing retards the extent to which aggregates are formed.

In summary, the aggregation process occurring in WB 2K-PUR reactive dispersions promotes uniform film formation by minimizing the extent to which macrophase separation of individual components occurs during film formation. If polyols become adsorbed to the surface of NCO droplets, a nano-dispersed phase morphology is essentially 'locked' into place via aggregation. Subsequently, when films are applied immediately after mixing, insufficient adsorption of polyol and/or self-crosslinking of NCO can facilitate bulk phase separation and de-wetting behavior at the F–A interface. This is precisely what was observed in the AFM images shown in Fig. 4.

5. Conclusions

These studies show that WB 2K-PUR reactive dispersions have a complex solution morphology that undergoes a number of parallel processes in the aqueous state before film formation. The proposed model based on experimental evidence involves the diffusion of water into WDPI reactant droplets, which leads to instability of dispersed polyol droplets and subsequent aggregation of reactant droplets ultimately resulting in gellation of the system at extended times. However, aggregation can be somewhat subdued by constant mixing of the aqueous reactive dispersions, which serves to partially reverse the aggregation process. While there has always been concern regarding the reactions of NCO groups with water in such systems, we have observed that, contrary to what might seem logical, for optimum gloss, it is beneficial to prolong the time after mixing of individual components before film formation, especially under high RH conditions.

Acknowledgements

A partial support from the National Science Foundation Materials Research Science and Engineering Center (MRSEC) Program (DMR 023883) through the REU program as well as Instrumentation Program (DMR-0315637) is also acknowledged. Bayer Corporation is acknowledged for supplying materials used in these studies.

References

[1] O'Sickey MJ, Lawrey BD, Wilkes GL. J Appl Polym Sci 2003;89:3520–9.
[2] O'Sickey MJ, Lawrey BD, Wilkes GL. Polymer 2002;43:7399–408.
[3] O'Sickey MJ, Lawrey BD, Wilkes GL. J Appl Polym Sci 2002;84:229–43.
[4] Velankar S, Cooper SL. Macromolecules 1998;31:9181–92.
[5] Velankar S, Cooper SL. Macromolecules 2000;33:395–403.
[6] Velankar S, Cooper SL. Macromolecules 2000;33:382–94.
[7] Coleman MM, Lee KH, Skrovanek DJ, Painter PC. Macromolecules 1986;19:2149–57.
[8] Coleman MM, Skrovanek DJ, Hu J, Painter PC. Macromolecules 1988;21:59–65.
[9] Painter PC, Park Y, Coleman MM. Macromolecules 1988;21:66–72.
[10] Garrett JT, Siedlecki CA, Runt J. Macromolecules 2001;34:7066–70.
[11] Garrett JT, Lin JS, Runt J. Macromolecules 2002;35:161–8.
[12] Rightor EG, Urquhart SG, Hitchcock AP, Ade H, Smith AP, Mitchell GE, et al. Macromolecules 2002;35:5873–82.
[13] Lee HS, Wang YK, MacKnight WJ, Hsu SL. Macromolecules 1988;21:270–3.
[14] Lee HS, Hsu SL. Macromolecules 1989;22:1100–5.
[15] Tao HJ, Meuse CW, Yang X, MacKnight WJ, Hsu SL. Macromolecules 1994;27:7146–51.
[16] Otts DB, Dutta S, Zhang P, Smith OW, Thames SF, Urban MW. Polymer 2004;45:6235–43.
[17] Barrere M, Landfester K. Macromolecules 2003;36:5119–25.
[18] Kaminski AM, Urban MW. J Coat Technol 1997;69:113–21.
[19] Otts DB, Urban MW. Polym Prepr 2003;44:105–6.
[20] Otts DB, Urban MW. Proceedings of the international waterborne, high-solids, and powder coatings symposium, New Orleans, USA. 30th ed 2003. p. 365–74.
[21] Otts DB, Urban MW. Polym Mater Sci Eng 2003;88:463–4.
[22] Otts DB, Urban MW. Polymer 2005, in press.
[23] Otts DB, Cueva-Parra LA, Pandey RB, Urban MW. Langmuir, 2005.
[24] Otts DB, Urban MW. Polym Mater Sci Eng 2004;91:765–6.
[25] Pandey RB, Urban MW. Langmuir 2004;20:2970–4.
[26] Urban MW, Allison CL, Finch CC, Tatro BA. J Coat Technol 1999;71:75–85.
[27] Urban MW, Allison CL. J Coat Technol 1999;71:73–8.
[28] Hoye TR, Eklov BM, Ryba TD, Voloshin M, Yao LJ. Org Lett 2004;6:953–6.
[29] Carr HY, Purcell EM. Phys Rev 1954;94:630.
[30] Meiboom S, Gill D. Rev Sci Instrum 1958;29:688.
[31] Dvorchak M. J Coat Technol 1997;69:47–52.
[32] Wicks ZW, Wicks DA, Rosthauser JW. Prog Org Coat 2002;44:161–83.
[33] Delides C, Pethrick RA, Cunliffe AV, Klein PG. Polymer 1981;22:1205.
[34] Lu X, Wang Y, Wu X. Polymer 1994;35:2315.
[35] Pegoraro M, Galbiati A, Ricca G. J Appl Polym Sci 2003;87:347–57.
[36] Zhang S, Cheng L, Hu. J Appl Polym Sci 2003;90:257–60.
[37] Dust JM, Fang ZH, Harris JM. Macromolecules 1990;23:3742–6.
[38] Heald CR, Stolnik S, Kujawinski KS, De Matteis C, Garnett MC, Illum L, et al. Langmuir 2002;18:3669–75.
[39] March J. Advanced organic Chemistry. 4th ed. New York: Wiley-Interscience; 1992.
[40] Harned HS, Davis Jr R. J Am Chem Soc 1943;65:2030–7.